ACCOUNTS of chemical research

Article

Cite This: Acc. Chem. Res. XXXX, XXX, XXX−XXX

pubs.acs.org/accounts

Carbon Nanodots for Charge-Transfer Processes

Published as part of the Accounts of Chemical Research special issue "Advanced Molecular Nanocarbons".

Alejandro Cadranel,[†,∇] Johannes T. Margraf,[§,∇] Volker Strauss,[∥,∇] Timothy Clark,[⊥] and Dirk M. Guldi*[,#]

[†]Departamento de Química Inorgánica, Analítica y Química Física, INQUIMAE, Facultad de Ciencias Exactas y Naturales, Universidad de Buenos Aires, Pabellón 2, Ciudad Universitaria, C1428EHA Buenos Aires, Argentina

[§]Chair for Theoretical Chemistry, Technische Universität München, Lichtenbergstr. 4, D-85747 Garching, Germany

[∥]Max Planck Institut für Kolloid- und Grenzflächenforschung, Am Mühlenberg 1, 14476 Potsdam, Germany

[⊥]Computer-Chemie-Centrum, Department of Chemistry and Pharmacy, Friedrich-Alexander-University Erlangen-Nürnberg, Nägelsbachstrasse 25, 91052 Erlangen, Germany

[#]Department of Chemistry and Pharmacy & Interdisciplinary Center for Molecular Materials, Friedrich-Alexander-University Erlangen-Nürnberg, Egerlandstrasse 4, 91058 Erlangen, Germany

CONSPECTUS: In recent years, carbon nanodots (CNDs) have emerged as an environmentally friendly, biocompatible, and inexpensive class of material, whose features sparked interest for a wide range of applications. Most notable is their photoactivity, as exemplified by their strong luminescence. Consequently, CNDs are currently being investigated as active components in photocatalysis, sensing, and optoelectronics. Charge-transfer interactions are common to all these areas. It is therefore essential to be able to fine-tune both the electronic structure of CNDs and the electronic communication in CND-based functional materials.

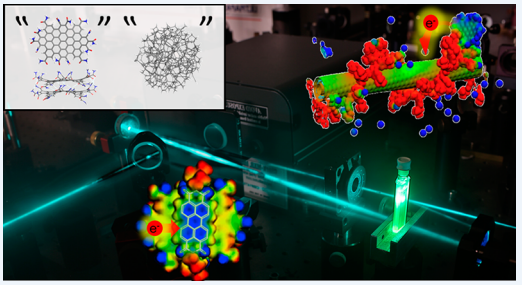

The complex, but not completely deciphered, structure of CNDs necessitates, however, a multifaceted strategy to investigate their fundamental electronic structure and to establish structure−property relationships. Such investigations require a combination of spectroscopic methods, such as ultrafast transient absorption and fluorescence up-conversion techniques, electrochemistry, and modeling of CNDs, both in the absence and presence of other photoactive materials. Only a sound understanding of the dynamics of charge transfer, charge shift, charge transport, etc., with and without light makes much-needed improvements in, for example, photocatalytic processes, in which CNDs are used as either photosensitizers or catalytic centers, possible.

This Account addresses the structural, photophysical, and electrochemical properties of CNDs, in general, and the charge-transfer chemistry of CNDs, in particular. Pressure-synthesized CNDs (pCNDs), for which citric acid and urea are used as inexpensive and biobased precursor materials, lie at the center of attention. A simple microwave-assisted thermolytic reaction, performed in sealed vessels, yields pCNDs with a fairly homogeneous size distribution of ∼1−2 nm. The narrow and excitation-independent photoluminescence of pCNDs contrasts with that seen in CNDs synthesized by other techniques, making pCNDs optimal for in-depth physicochemical analyses. The atomistic and electronic structures of CNDs were also analyzed by quantum chemical modeling approaches that led to a range of possible structures, ranging from heavily functionalized, graphene-like structures to disordered amorphous particles containing small sp^2 domains.

Both the electron-accepting and -donating performances of CNDs make the charge-transfer chemistry of CNDs rather versatile. Both covalent and noncovalent synthetic approaches have been explored, resulting in architectures of various sizes. CNDs, for example, have been combined with molecular materials ranging from electron-donating porphyrins and extended tetrathiafulvalenes to electron-accepting perylendiimides, or nanocarbon materials such as polymer-wrapped single-walled carbon nanotubes. In every case, charge-separated states formed as part of the reaction cascades initiated by photoexcitation. Charge-transfer assemblies including CNDs have also played a role in technological applications: for example, a proof-of-concept dye-sensitized solar cell was designed and tested, in which CNDs were adsorbed on the surface of mesoporous anatase TiO_2. The wide range of reported electron-donor−acceptor systems documents the versatility of CNDs as molecular building blocks, whose electronic properties are tunable for the needs of emerging technologies.

INTRODUCTION

Carbon-based functional materials have lain in the focal point of enormous research efforts in the past few decades. The systematic extension of the nanocarbon family resulted from

Received: December 29, 2018

DOI: 10.1021/acs.accounts.8b00673
Acc. Chem. Res. XXXX, XXX, XXX−XXX

continuous research on functional nanocarbons and their integration into functional devices. One branch of this family tree, photoluminescent carbon-based nanoparticles, has grown considerably in the past 12 years.[1] Strictly speaking, these particles are nanocarbon derivatives with (partially) amorphous structures and a high heteroatom content. Catalysis, sensing, imaging, lighting, drug delivery, and solar-energy conversion are just a few areas in which they show great promise.

As for many other nanocarbons, commercialization of carbon nanodots (CNDs)-based products has been hampered by poor control over their structure and electronic properties. Precise structural characterization constitutes a great challenge. Attempts have been made to classify carbon-based nanoparticles according to their structure and/or synthetic route. One of these attempts, introduced by Cayuela et al. in 2016, is based on the categorization of carbon-based nanoparticles according to not only their structure but also their electronic deactivation.[2] A controversial debate as to whether the electronic deactivation in bottom-up synthesized carbon-based particles is subject to any sort of quantum confinement has ensued: Compelling evidence suggests that the photoluminescence (PL) has several different origins, and a conclusive assignment is difficult. Nanocarbon materials of variable sizes and properties can be obtained, depending on the reaction conditions, in one and the same reaction. The presence of heteroatoms and the vast variety of structural features have led to the suggested designations "carbon-based nanoparticles" or "carbogenic dots".[3] Terms such as CNDs or "carbon dots (CDs)", nevertheless, are widely used; none of them implies any intrinsic physical process, such as quantum confinement, or structural features, such as a two-dimensional (2D) or layered spectroscopies suggest.

A number of review articles covering general aspects regarding CNDs, graphene quantum dots (GQD), etc., in which synthesis and applications lie at the forefront, have been published in recent years.[4−11] Specific aspects, of which major developments of CNDs in photocatalysis is a leading example, have also been reviewed in the literature.[12,13] Charge-transfer properties of CNDs have been concluded to be largely unexplored territory: "[···] *direct evidence and essence of the photoinduced charge separation in CQDs have not been accomplished*".[12] This Account fills this charge-transfer gap by documenting evidence of charge transfer with CNDs upon photoexcitation obtained in our laboratory over the past five years. To place our work on tuning charge transfer in CNDs into the right context, we will first highlight our own efforts to elucidate the electronic structure of prototype CNDs. We will then put our work into perspective with respect to current research on CNDs in charge-transfer applications as it reaches out into many other fields.

Photophysical Properties of CNDs

PL in functionalized or defect-rich carbon materials is very common. For example, strong PL evolved in multiwalled carbon nanotubes in the visible range upon cutting them into small fragments and oxidizing to yield a large number of carboxylic groups.[14] Likewise, PL is observed in carbon nano-onions and hydrogenated graphene.[15,16] In the latter, sp^2-conjugated domains on the order of a few nanometers are electronically isolated by largely hydrogenated areas, so that PL was described in hydrogenated carbon films in numerous publications from the 1990s.[17−19]

The concept of photoluminescent CNDs was raised in 2006 by Sun et al., following their earlier observation of luminescent carbon-based particles during laser ablation of a carbon source in the presence of water.[20,21] Their simple synthesis and ease of handling has led to a rapidly rising interest in studying the formation, the properties, and the applications of CNDs. Bottom-up synthesized CNDs are of particular interest, as they can be produced from natural resources without the comparatively expensive oxidation of mineral graphite or the use of crude oil-based starting materials. Furthermore, a careful selection of the synthesis parameters enables structure and size and, subsequently, optical and electrochemical properties to be tuned.[22,23]

A widely employed and studied precursor system is citric acid/urea (CA/U).[24] CA/U-based CNDs are produced in a simple microwave-assisted thermolytic reaction in H_2O or other polar solvents. The CA/U system was first described in 1893.[25] The light brown product obtained in the thermal reaction of CA and U was named "citrazinamide" and was shown to fluoresce in solution. CA/U systems have numerous advantages that range from the use of inexpensive, biobased starting materials to the ability to tune the PL to some degree.[22,23] Interpretations of their structure and reactivity, especially regarding structure−property relationships, should be treated with caution due to the heterogeneous and reactive nature of the CND products. However, conducting the reaction in a sealed vessel and under pressure resulted in small (∼1−2 nm) homogeneously distributed CNDs.[26] Higher PL quantum yields were also realized in this manner. Structural characterization by, for example, transmission electron microscopy (TEM) and powder X-ray diffraction (XRD), reveals the presence of heavily functionalized π-conjugated particles. Note that very small particles with highly amorphous structures are unlikely to be detectable in TEM. In the case of pressure synthesized CNDs (pCNDs), atomic force microscopy and UV/vis analytical ultracentrifugation reveal a mean size of ∼1−2 nm and a maximum size of 4 nm.[27]

By far the most intriguing property of CNDs is their PL, although its exact origin is subject to controversial debate. pCNDs display a narrow, excitation-independent PL (Figure 1),

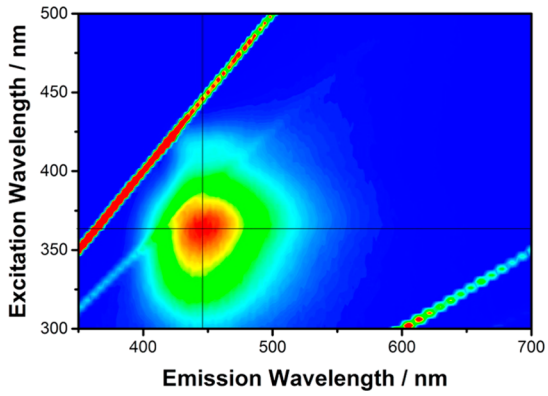

Figure 1. Three-dimensional PL plot of pCND in aqueous solutions at room temperature with increasing intensity from blue to green and to red.

which indicates that pCNDs emission is originated in a single particle species and that pCNDs are a homogeneous material in terms of their molecular structure. This motivated us to investigate the underlying electronic deactivation mechanism. Time-resolved techniques, such as time-correlated single-photon counting (TCSPC), fluorescence up-conversion spec-

DOI: 10.1021/acs.accounts.8b00673
Acc. Chem. Res. XXXX, XXX, XXX−XXX

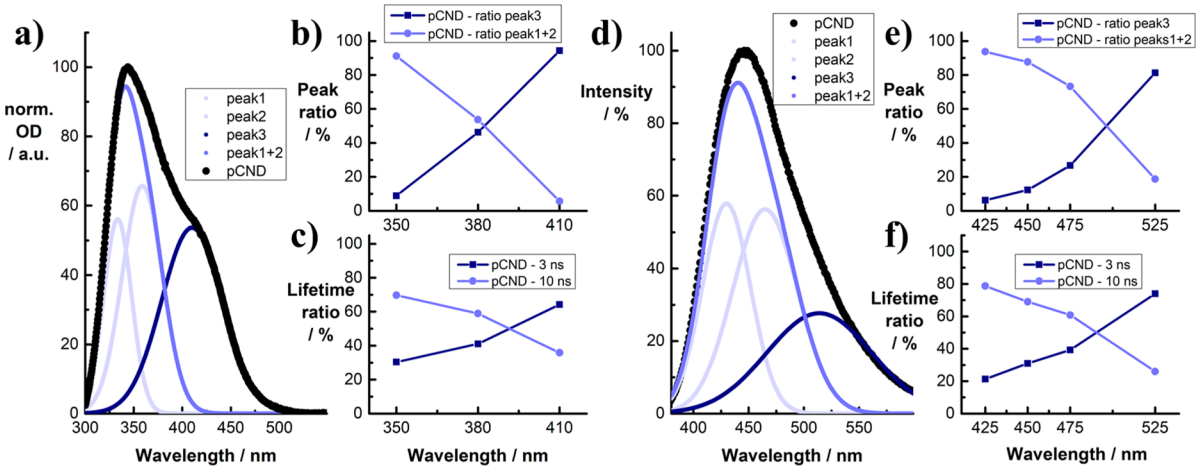

Figure 2. (a) Multiple curve fitting of the absorption spectrum of pCNDs in H_2O. (b) Relative peak intensities for different excitation wavelengths. (c) Relative distribution of lifetimes at different excitation wavelengths. (d) Multiple curve fitting of the fluorescence spectrum of pCNDs in H_2O upon 350 nm excitation. (e) Relative peak intensities for different wavelengths. (f) Relative distribution of lifetimes at different emission wavelengths.

troscopy (FLUPS), and transient absorption spectroscopy (TAS), were used to probe their excited-state deactivation.

A complex deactivation mechanism based on a number of electronic processes governs the PL of CNDs. For example, a fast deactivation in the low picosecond regime that occurs within the sp^2-conjugated domains (the core) is seen at higher energies (toward the blue end). A slower deactivation in the short nanosecond regime takes place at the red end of the features and is assigned to electronic processes mediated by surface groups, like in inorganic QDs with surface traps. In small and/or more amorphous CNDs, the slow deactivation, which dominates the PL, is due to the presence of a larger number of surface states. Experimental confirmation came from a combination of FLUPS and TCSPC.[27]

Excitation-dependent PL is taken to indicate trap states, from which different deactivation lifetimes originate. A clear relationship exists between surface states and optical features of CNDs. PL lifetime measurements of CNDs yield two major components that evolve in different energy regions. Steady-state excitation and emission wavelength-dependent measurements correlated with the PL lifetimes revealed that the absorption and PL spectra are best described as the superimpositions of several electronic transitions.[28] Multiple peak fitting showed that some photoluminescent surface states are bimodal, while others are monomodal (Figure 2). A combined spectro-electrochemical analysis, in which specific optical features were quenched upon applying reducing and/or oxidizing potentials, confirmed this conclusion. These experiments were all intended to correlate the optical and electrochemical reduction and/or oxidation.

The exact structure from which the surface-state related PL originates is still not clear. The PL quantum yields of these surface states are higher than those from the core and are prone to photobleaching. For example, the PL of CNDs synthesized in a thermal reaction under pressure depends on the reaction temperature and/or time.[29] PL quantum yields tend to be higher for CNDs synthesized at lower temperatures of ~180 °C.[26] At temperatures higher than 200 °C, reduction of surface traps/functionalities is observed, along with an increase of features related to the sp^2-conjugated core. In general, at elevated temperatures and under exclusion of oxygen, the surface traps/functionalities are constantly removed, leading to a loss of mass of 50%−60% and greater than 70% carbon.[27,30] PL is still detectable for such (defunctionalized) CNDs with, however, significantly lower quantum yields.

Pyridones are a likely surface-located trap/functionality and are responsible for the multitude of electronic transitions observed in CNDs.[26] Differences in terms of reactivity under pressure and, in turn, different reaction mechanisms may lead to variations in CND size and traps/functionalities. Such a hypothesis is in sound agreement with the observation that the PL quantum yields scale with the effective nitrogen loading in CNDs.[31]

Currently, the unambiguous interpretation of the spectroscopic results has been hampered by insufficient structural characterization of CNDs. Computational modeling has evolved as a powerful tool; it allows the construction of models with clear structure−property relationships. In the absence of compelling evidence, it is, however, important to compare different possible structural architectures. Three different structures have mainly been considered in the literature (Figure 3). First, CNDs are at

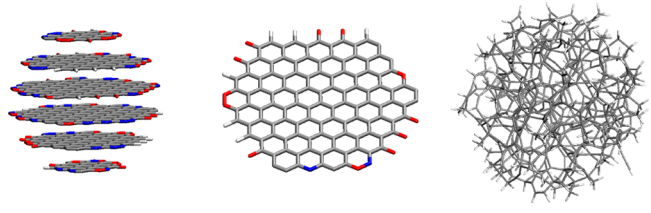

Figure 3. Illustration of commonly proposed CND structure types: Spherical, graphitic particles (left), 2D, graphene-like nanosheets (center) and disordered, amorphous structures (right).

times represented as spherical, graphitic particles. Second, they are often modeled as 2D, graphene-like structures. Third, they are considered as disordered, amorphous structures, with small embedded sp^2-conjugated domains.[2]

Spherical, graphitic particles are unlikely to be a physically relevant model for highly photoluminescent, bottom-up synthesized CNDs. On the one hand, such graphitic structures would not feature a band gap/PL and, on the other hand, they would be insoluble, especially in polar media such as water. 2D, graphene-like nanosheets may display these properties if they are small (1−2 nm) and peripherally functionalized with, for

DOI: 10.1021/acs.accounts.8b00673
Acc. Chem. Res. XXXX, XXX, XXX−XXX

example, carboxylic acid groups. They are the model used most frequently to study the electronic properties of CNDs. Models based on disordered, amorphous structures have been considered far less often, mainly because it is difficult to define amorphous structures. We reported a library of such structures determined from a melt/quench procedure, in which randomized periodic carbon structures were generated and then quenched to the next local minimum, iterating hundreds of times.[31]

IR and Raman spectroscopy suggests that CNDs are far from perfect 2D crystals and that they feature a high degree of peripheral functionalization and structural defects. Thus, 2D, graphene-like nanoflakes and disordered, amorphous structures represent the two extreme ends of the spectrum of possible CND structures. Both steady-state and time-resolved optical spectroscopies point to the coexistence of multiple electronic states within single particles. This resembles what is observed for inorganic QDs with surface defects. In graphene-like structures, surface states are typically associated with edge terminations. Interestingly, we found that amorphous structures display the same qualitative features (see Figure 4). Here, the surface states correspond to small organic chromophores (i.e., sp^2-conjugated domains) embedded in an amorphous matrix.

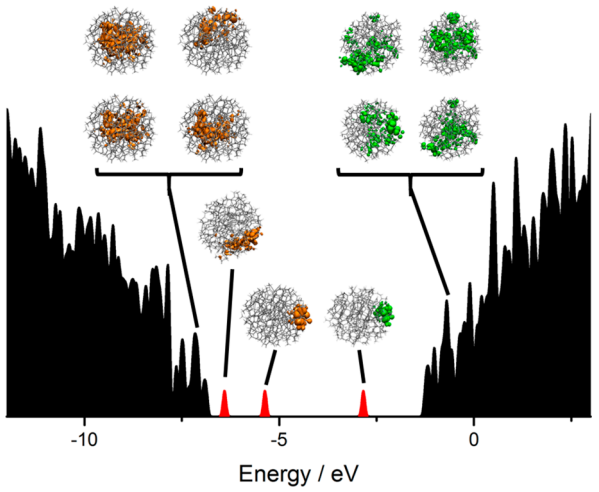

Figure 4. Calculated density of states for disordered, amorphous CND models, featuring a broad continuum of delocalized, band-like states (black) and individual localized surface states (highlighted in red).

The notion of largely amorphous structures containing aromatic domains has been confirmed in experimental models, in which polyaromatic hydrocarbons such as anthracene were embedded in inert polymer matrices.[32] Tuning of the latter led to a remarkable resemblance with the CND optical properties. Overall, theoretical and experimental evidence suggests that the optical CND properties stem mainly from localized features. Optically active constituents may consist of both larger sp^2-conjugated carbon domains and smaller heteroatom-containing molecular chromophores: Several structural moieties have been discussed, including anthracene, pyridine, pyridone, etc.[26,32,33] In the bigger picture, the coexistence of different active sites in a single CND contributes to the complex exciton relaxation dynamics and excitation-wavelength dependent PL. CND optical properties are governed by the type and amount of electroactive structural sites: A clear indication of this is the large variation of CNDs obtained by even slight changes in the synthetic parameters.

Their multitude of electronic states makes CNDs an emerging platform for diverse applications in charge-transfer schemes. In early CND work on charge-transfer interactions, the PL was found to be quenched in the presence of both electron donors and acceptors.[34] Our steady-state and time-resolved spectroscopic assays showed that such PL quenching is based on charge-transfer reactions in the excited state. Important charge-transfer parameters include the underlying binding motifs and the electron-donor and/or -acceptor strengths. For example, the PL quenching rate is almost 2 orders of magnitude higher for charged electron acceptors than for uncharged molecular electron donors (Figure 5a,b,d,e).[27] Spectro-electrochemical and pulse-radiolytic experiments on CNDs showed that specific features respond at different potentials upon electrochemical reduction and/or oxidation (Figure 5c,f).[28]

Charge-Transfer Properties

One of the most striking features of CNDs is their charge-transfer chemistry; they serve as either electron donors or acceptors. Many supramolecular architectures of different sizes have been designed by combining CNDs with molecular and particulate building blocks or mesoporous surfaces. They operate via charge transfer to or from photoexcited CNDs. Overall, CNDs have evolved as versatile building blocks for supramolecular architectures with tailored electronic properties, suggesting the use of CNDs in technological devices that require cheap materials with charge-transfer activity.

CNDs as Electron Acceptors

The electron-accepting character of CNDs was explored in combination with, for example, electron-donating porphyrins and π-extended tetrathiafulvalene (exTTF). Porphyrins were selected because of their planar 18-π-electron aromatic structure, which ensures high molar extinction coefficients and efficient pathways for energy- and charge-transfer events. Moreover, a broad range of peripheral functionalization allows their redox potentials to be fine-tuned,[35] while enabling them to participate in noncovalent, supramolecular architectures, and to be incorporated in covalently linked electron donor−acceptor conjugates. In contrast, the pro-aromatic exTTF[36] gains planarity and aromaticity upon one- and two-electron oxidation. This results in the formation of stable oxidized forms at relatively moderate potentials and facilitates charge-transfer events.

In a well-defined covalent porphyrin-CND electron donor−acceptor conjugate, the amino groups of nitrogen-doped CNDs (nCNDs), reminiscent of the ethylenediamine precursor, were targeted in a coupling reaction with a carboxyphenyl-functionalized porphyrin (Figure 6a).[37] Appreciable nCND-porphyrin ground-state interactions induce both red shifts and broadening of the Soret- and Q-band absorptions in comparison to reference porphyrin and blue-shifted nCND-absorptions. Excited-state interactions result in a substantial quenching of emissions for the electron donor−acceptor conjugate compared to its individual constituents. Selective nCND excitation at 300 nm initiates an energy-transfer process to the covalently attached porphyrin, leading to porphyrin fluorescence. Likewise, selective excitation of the porphyrin at 422 nm is followed by red shifts from 645 and 715 nm to 651 and 721 nm in the electron donor−acceptor conjugate, accompanied by a sizable fluorescence quenching (Figure 6b). Ultrafast TAS revealed a transient spectrum remarkably similar to the sum of the one-electron reduced nCND and the one-electron oxidized porphyrin, suggesting that charge separation and recombination are responsible for the excited-state deactivation of the nCND-porphyrin. Charge

DOI: 10.1021/acs.accounts.8b00673
Acc. Chem. Res. XXXX, XXX, XXX−XXX

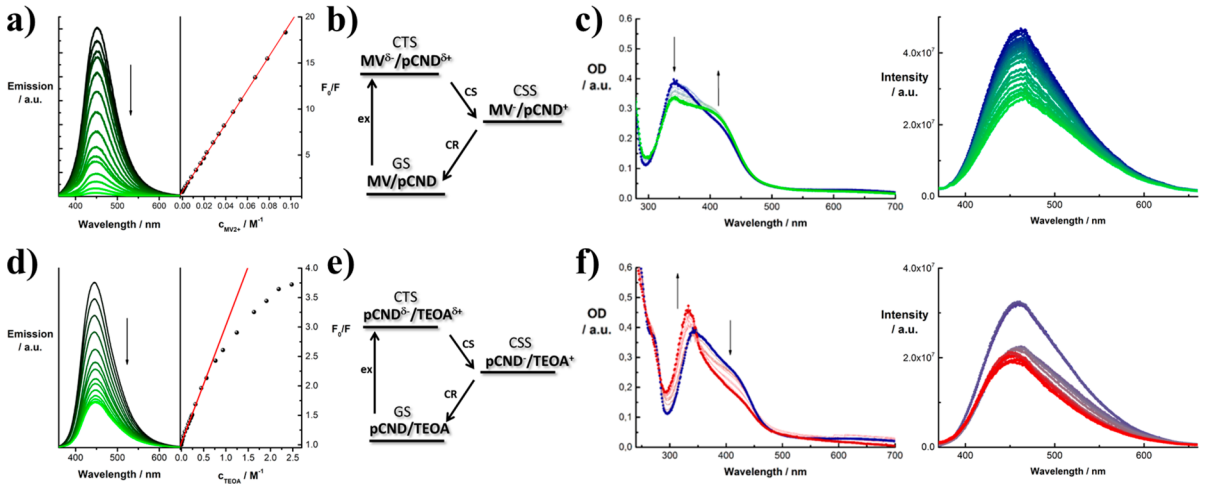

Figure 5. (a) (left) Steady-state emission spectra of pCND with increasing amounts of methylviologen (MV^{2+}) upon excitation at 350 nm. (right) Corresponding Stern–Volmer plot. (b) Energy diagram illustrating the excited-state deactivation. (c) UV–Vis absorption (left) and emission (right) spectra of pCNDs in H_2O with 0.1 M $TBABF_4$ as supporting electrolyte when screening potentials from 0 to +1.5 V (blue to green). (d) (Left) Steady-state emission spectra of pCND with increasing amounts of triethanolamine (TEOA) upon excitation at 350 nm. (Right) Corresponding Stern–Volmer plot. (e) Energy diagram illustrating the excited-state deactivation; (f) UV–vis absorption (left) and emission (right) spectra of pCNDs in H_2O with 0.1 M $TBABF_4$ as supporting electrolyte when screening potentials from 0 to −1.5 V (blue to red).

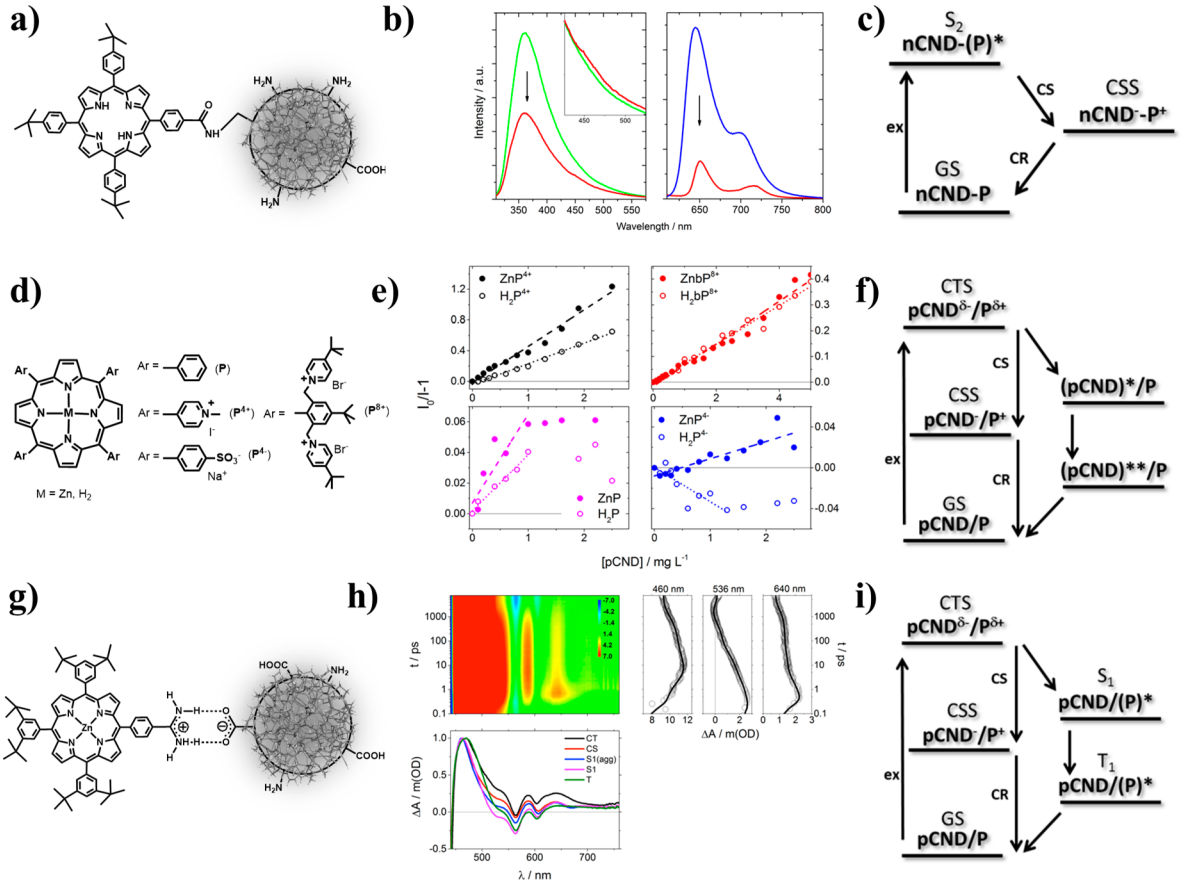

Figure 6. (a) Structure of the covalent electron donor–acceptor conjugate between nCNDs and tetraarylporphyrin. (b) Fluorescence spectra of the reference porphyrin (blue), nCNDs (green), and the nCND-P (red). (c) Energy diagram illustrating the excited-state deactivation. (d) Structure of the porphyrins studied in noncovalent electron-donor–acceptor systems with pCNDs. (e) Stern–Volmer plots for the emission quenching of ZnP^{4+} and H_2P^{4+} (upper left), ZnP^{8+} and H_2P^{8+} (upper right), ZnP and H_2P (bottom left), and ZnP^{4-} and H_2P^{4-} (bottom right) upon the addition of pCNDs. (f) Energy diagram illustrating the excited-state deactivation. (g) Structure of the H-bonded electron donor–acceptor between pCND and tetraarylporphyrin. (h) Differential absorption 3D map obtained from TAS (λ_{ex} = 420 nm), time-absorption profiles (open circles), and global analysis fittings (solid lines), and normalized decay-associated spectra showing a charge-transfer (CT) and a charge-separated (CS) state. (i) Energy diagram illustrating the excited-state deactivation.

DOI: 10.1021/acs.accounts.8b00673
Acc. Chem. Res. XXXX, XXX, XXX–XXX

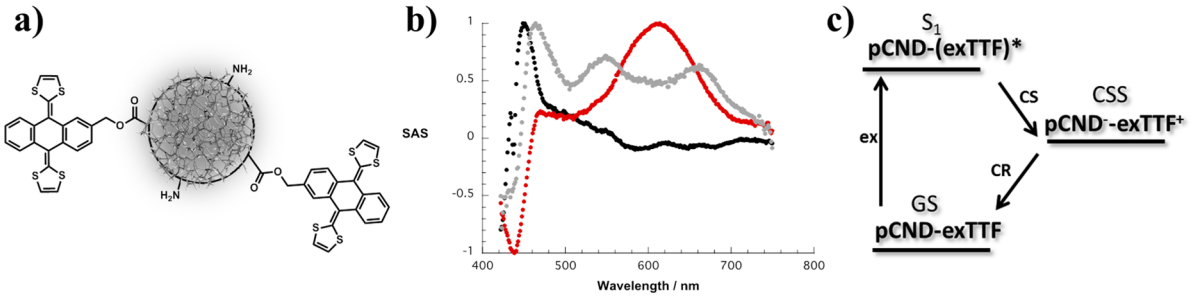

Figure 7. (a) Structure of the covalent electron-donor–acceptor conjugate between pCNDs and exTTF. (b) Normalized decay associated spectra showing an exTTF-centered excited-state (red) and a charge-separated state (gray). (c) Energy diagram illustrating the excited-state deactivation.

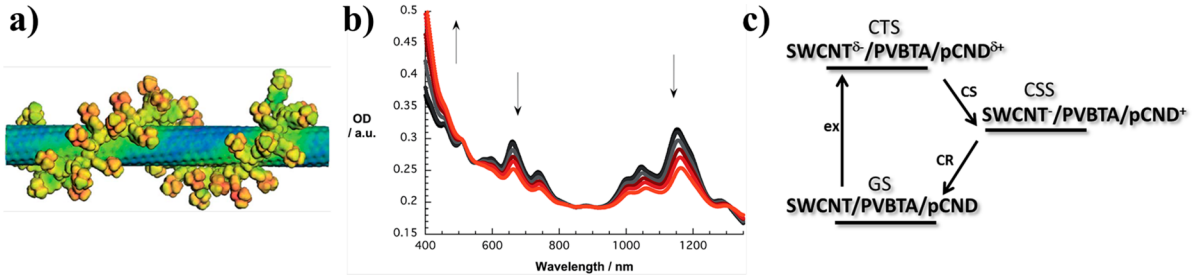

Figure 8. (a) Plot of the molecular electrostatic potential on a 0.03 e^{-} $Å^{-3}$ electron density isosurface of the SWCNT/PVBTA system with Cl^{-} counterions. (b) Absorption spectra recorded over the course of sequential addition of pCNDs to SWCNT/PVBTA. (c) Energy diagram illustrating the excited-state deactivation.

recombination leads to ground-state recovery in a biphasic process with lifetimes of 6.3 and 225 ps (Figure 6c).

As a complement, noncovalent interactions were tested in a series of porphyrins featuring diverse functionalities in their *meso*-positions.[35] For example, metalated versus nonmetalated, positively versus negatively charged, and neutral versus bulky porphyrins were essayed with pCNDs (Figure 6d), for which negative ζ-potentials in various solvents indicate a negatively charged surface. Spectrophotometric titrations revealed that the addition of pCNDs to solutions of the positively charged porphyrins caused an intensity decrease and a red shift of the Soret-band absorption that ranges between 2 to 9 nm. In stark contrast, no appreciable changes were detected for neutral or negatively charged porphyrins. Similar observations were made in the fluorescence experiments, in which titrations of the positively charged porphyrins with pCNDs afforded up to 90% quenching of the porphyrin fluorescence and Stern–Volmer constants up to 0.48 mg^{-1} L. TAS supports the notion that a charge-transfer state is populated through excitation. It decays in a parallel branching and affords, on the one hand, a charge-separated state and, on the other hand, a pCND-centered state (Figure 6f). From the former, charge recombination occurs in the range from 18 to 37 ps and depends on the nature of the porphyrin. Reference measurements with neutral or negatively charged porphyrins proved to be very important. They support the hypothesis that electrostatic forces are essential for the formation of the supramolecular architectures (Figure 6e). A sizable cooperation from π-stacking was also noted: For the bulky, positively charged porphyrins, Soret- and Q-band absorption red-shifts are smaller, and fluorescence quenching is reduced from 90% to 60%. Stern–Volmer constants also diminish from 0.48 to 0.083 mg^{-1} L. Coordination, however, contributes only to a minor extent, as metalated porphyrins show stronger quenching than nonmetalated ones. Interestingly, for bulky porphyrins, where coordination is sterically impeded, metalated and nonmetalated porphyrins behave more or less the same (Figure 6e).

The focus was different when amidine-functionalized porphyrins were used. They were designed to support H-bonding interactions and the formation of salt bridges with the carboxylates of pCNDs (Figure 6g).[38] H-Bonded architectures with charge-transfer activity were verified in anhydrous dimethylformamide (DMF), although the red shift of the Soret-band absorption was only 1 nm. Fluorescence quenching reached ~15% of the initial intensity. Stern–Volmer constants for emission quenching (0.088 mg^{-1} L) resemble those obtained for the positively charged porphyrins. Additionally, charge separation and recombination take place upon photoexcitation with 2 and 27 ps, respectively (Figure 6h,i). Interestingly, no H-bonding interactions could be verified in the presence of water, probably due to solvent molecules blocking the salt-bridge formation.

An exTTF donor was also incorporated into covalent electron donor–acceptor conjugates with pCNDs.[36] pCNDs were reacted with thionyl chloride and subsequently with hydroxymethyl-exTTF to afford pCND-exTTF (Figure 7a). In pCND-exTTF, ground-state electronic interactions are not evident, since, for example, the absorption features and the one-electron oxidation of exTTF remained unchanged relative to the reference. Nevertheless, an emission quenching of over 90% was found. This quenching goes along with a TAS transient upon 387 nm photoexcitation, which showed the fingerprints of the one-electron oxidized form of exTTF (Figure 7b); a charge separation that takes ~1.3 ps is responsible before the ground state is reinstated via charge recombination in 13.3 ps (Figure 7c).

CNDs as Electron Donors

To shed light onto the electron-donating characteristics of CNDs rather than their electron-accepting characteristics, the focus was shifted to several classes of electron acceptors, namely,

DOI: 10.1021/acs.accounts.8b00673
Acc. Chem. Res. XXXX, XXX, XXX–XXX

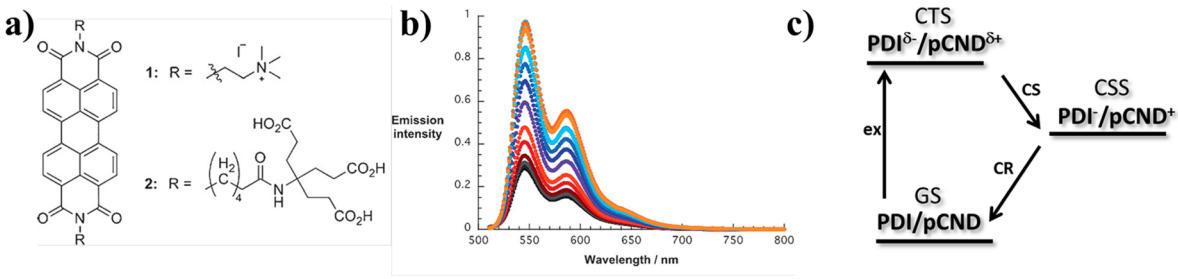

Figure 9. (a) Structure of the PDIs studied in noncovalent hybrids with pCNDs. (b) Fluorescence spectra of 1 (black) during the course of a titration with pCND (red > blue > orange). (c) Energy diagram illustrating the excited-state deactivation.

ionic polymer-wrapped single-walled carbon nanotubes (SWCNT) and perylenediimides (PDI). In both cases, a noncovalent approach was pursued to keep the electronic structure of both donor and acceptor largely unperturbed. The selected structures display several highly attractive features. When doped, SWCNTs with their high charge-carrier mobilities give rise to enhanced light absorption, charge separation, and transport with either electron donors or acceptors in comparison to pristine SWCNT.[39] Meanwhile, PDIs represent a unique class of molecular acceptors, due to their π-extended planar aromatic structure and the many possibilities of functionalization at the bay and imide positions.

SWCNTs were wrapped with the positively charged poly(4-vinylbenzyl)trimethylamine (PVBTA) by means of hydrophobic interactions. In the next step, negatively charged pCNDs were immobilized onto the surface of the SWCNT/PVBTA using electrostatic attractions to generate a three-component SWCNT/PVBTA/pCND electron donor−acceptor system (Figure 8a).[39] Absorption titrations of (SWCNT/PVBTA)s with pCNDs display large red shifts of up to 15 nm for the S_{11} and up to 4 nm of the S_{22} transitions (Figure 8b). Charge-transfer interactions in the ground state are suggested by these shifts. Similar red shifts were also observed in fluorescence titrations upon SWCNT excitation. The latter goes hand-in-hand with a significant overall quenching of the SWCNT-NIR fluorescence. To the same extent, in reverse titration experiments pCND emission was monitored when (SWCNT/PVBTA)s was added to constant amounts of pCND. In this particular case, the quenching was accompanied by an overall red shift up to a point at which a blue shift sets in. In short, excited-state interactions are rather complex in SWCNT/PVBTA/pCND. Molecular dynamics calculations support the notion that the underlying electronic interactions are not based on simple π-stacking. In TAS experiments, features of the reduced SWCNTs consistent with a charge separation are observed. Charge recombination with a lifetime of 105 ps rounds off the excited-state deactivation (Figure 8c).

Likewise, PDI/pCND systems were brought together by means of electrostatic interactions with PDIs bearing positively charged trimethylammonium functionalities (Figure 9a).[27] Formation of PDI/pCND results in a 33% decrease and a 4 nm red shift of the PDI-centered absorption upon addition of pCNDs. Moreover, 70% of the PDI-centered fluorescence intensity is quenched in titration experiments with pCNDs (Figure 9b), from which a Stern−Volmer constant of 0.025 mg^{-1} L was derived. In electrochemical titrations, the PDI reduction becomes more negative when pCNDs are present. A charge-density shift from the pCNDs to the PDI in the ground state is inferred.

Excited-state interactions parallel with the marked ground-state interactions result in a decrease of the PDI fluorescence lifetimes from 4.7 to 0.2 ns in the absence and presence of pCNDs, respectively. Notably, none of the aforementioned effects were observed when negatively charged carboxylate substituents, rather than positively charged trimethylammonium groups, were present on the PDI. In TAS experiments performed with PDI/pCND, the fingerprints of the one-electron reduced PDI were detected immediately after the 500 nm pump pulse. This points to charge separation as the main deactivation pathway. Charge recombination is biphasic, with lifetimes of 4 and 210 ps (Figure 9c).

Charge-Transfer of CNDs in Applications

The charge-transfer chemistry of CNDs, especially as electron donors, has also been exploited in promising materials for biomedical and/or energy applications. Supramolecular systems have been studied, in particular. For example, assemblies of gold nanoparticles and pCNDs (Au@pCND) were used as sensitizers in cancer radiotherapy. Additionally, CNDs made from urea, citric acid, and formic acid have been adsorbed onto mesoporous titania films and studied as sensitizers in dye-sensitized solar cells (DSSC).

pCNDs act as both reducing and stabilizing agents in Au@pCND.[40] In the resulting bulbous metallic nanoparticles, an amorphous carbon shell capped the gold core, as revealed by TEM. The absorption and emission spectra of Au@pCND show features assignable to oxidized pCNDs, while Fourier transform infrared (FTIR) spectroscopy confirms the presence of oxidized functional groups in the 1500 to 1700 cm^{-1} and the 1100 to 1450 cm^{-1} regions. Au@pCND were stabilized by charge-transfer interactions; confirmation also came from TAS experiments, where a significant contribution from charge-transfer interactions was observed. The Au@pCND clusters showed improved efficiency and biocompatibility in comparison to gold nanoparticles stabilized with citric acid.

Photoanodes for DSSCs were prepared by dipping mesoporous titania electrodes into HNO_3-acidified aqueous solutions of pCNDs for 6−8 h.[41] The cell setup was completed with a standard Pt counterelectrode and an electrolyte based on the I^-/I_3^- couple. A moderate efficiency of 0.24% was obtained. Lowering the pH of the aqueous pCND solutions results in an intensification of the IPCE spectra due to better surface coverage compared to photoanodes prepared at higher pH. The DSSC efficiency of pCND solar cells is, however, more than an order of magnitude smaller than that of dye-sensitized or inorganic QD solar cells. TAS experiments were used to investigate reasons for the poor performance with pCND-covered titania photoanodes; three lifetimes, on the time scales of 1, 10, and 100 ps, depending on the measurement conditions,

DOI: 10.1021/acs.accounts.8b00673
Acc. Chem. Res. XXXX, XXX, XXX−XXX

were determined. The first and second lifetimes were associated with nonradiative recombination processes and population of the trap states/charge injection into the titania conduction band, respectively, while the third lifetime was ascribed to charge recombination between the injected carriers and the oxidized pCNDs. Additional evidence for this interpretation comes from open-circuit voltage decays, obtained under pulsed LED illumination. These measurements confirmed that trap states, inherent to pCNDs, are an integral part of the decay cascades upon photoexcitation. Indeed, decreasing the density of trap states proved more beneficial for solar-cell performance than increasing the spectral range of light harvesting. This is because these excited states fail to contribute to the charge injection due to their ultrashort lifetimes. Overall, a rather poor balance between charge recombination and regeneration causes the moderate DSSC performance of pCND solar cells.

OUTLOOK

Charge-transfer processes play an important role in a wide range of applications for which CNDs have proved an interesting class of nanocarbon materials with high potential. In a number studies, we have provided compelling evidence for charge transfer in functional assemblies with CNDs, on the one hand, and molecular electron donors and acceptors, single-walled carbon nanotubes, gold nanoparticles, and anatase TiO_2, on the other hand. Fine-tuning the surface chemistry of CNDs allows them to be exploited as either electron donors or acceptors. A comprehensive correlation between the physicochemical properties and structural features is, however, complex. Our combined spectroscopic and electrochemical approach, which aims to correlate these features, can be regarded as a good starting point toward a wide-ranging understanding of the excited-state dynamics and a more efficient exploitation of charge carriers. Systematic spectro-electrochemical investigations, which will be based on a range of different CNDs, will be of utmost importance to gather an unambiguous interpretation of the structure−property relationships.

In general, charge transfer is key to many applications, such as photocatalysis, photosensing, or photosensitization. In fact, the good water solubility, low toxicity, and inexpensive nature of CNDs make one of the most interesting upcoming applications photocatalysis.[42−44] Investigating and understanding fundamental charge-transfer properties may lead to critical improvements of, for example, photocatalytic processes, in which CNDs are used as photosensitizers and/or catalytic centers. Therefore, a systematic improvement of the charge injection/electronic communication between CNDs and their current collectors or catalyst counterparts based on a combination of structural, photophysical, and electrochemical assays is pivotal.

AUTHOR INFORMATION

Corresponding Author

*E-mail: dirk.guldi@fau.de.

ORCID

Alejandro Cadranel: 0000-0002-6597-4397
Volker Strauss: 0000-0003-2619-6841
Timothy Clark: 0000-0001-7931-4659
Dirk M. Guldi: 0000-0002-3960-1765

Author Contributions

[▽]These authors equally contributed to this work

Notes

The authors declare no competing financial interest.

Biographies

Volker Strauss received his Ph.D. at the University of Erlangen-Nürnberg in Germany under the supervision of Prof. Dirk M. Guldi. He went on to pursue a German Research Foundation (DFG)-funded postdoctoral research with Prof. Richard B. Kaner at the University of California, Los Angeles. At present Volker is a group leader at the Max Planck Institute of Colloids and Interfaces in Potsdam. His work is dedicated to the investigation of functional carbon-based materials in catalysis and nanoelectronics.

Alejandro Cadranel obtained his Ph.D. degree at the University of Buenos Aires (UBA) in Argentina, under the supervision of Prof. Luis M. Baraldo. After a postdoctoral period at the same university with Prof. José H. Hodak, he joined Prof. Guldi's group at the University of Erlangen-Nürnberg as a postdoctoral researcher. Alejandro just moved back to Buenos Aires to join UBA and the national research council (CONICET). His research focuses on supramolecular photochemistry of donor−acceptor systems and coordination complexes for energy management and catalysis.

Johannes Margraf performed his doctoral studies at the University of Erlangen-Nürnberg in the groups of Tim Clark and Dirk Guldi, working on the theoretical and experimental characterization of nanomaterials. He subsequently moved on to a postdoctoral fellowship to work on electronic structure theory with Rodney Bartlett (at the Quantum Theory Project of the University of Florida), funded by the Humboldt Foundation. Currently, Johannes is working at the Technical University of Munich, where he studies complex reaction networks in catalysis.

ACKNOWLEDGMENTS

We gratefully thank all our collaborators that participated in the research covered in this article. V.S. was supported by the Deutsche Forschungsgemeinschaft (German Academic Research Society), Grant No. STR1508/3-1. A.C. acknowledges a postdoctoral scholarship from DAAD-ALEARG and is a member of ALN. J.T.M was supported by a Beilstein Foundation Fellowship. We also acknowledge support from the Deutsche Forschungsgemeinschaft—Project No. 182849149-SFB 953—and the Bavarian Ministry of Education, Culture, Science and Art as part of the *Solar Technologies go Hybrid* initiative.

REFERENCES

(1) Georgakilas, V.; Perman, J. a.; Tucek, J.; Zboril, R. Broad Family of Carbon Nanoallotropes: Classification, Chemistry, and Applications of Fullerenes, Carbon Dots, Nanotubes, Graphene, Nanodiamonds, and Combined Superstructures. *Chem. Rev.* **2015**, *115*, 4744−4822.

(2) Cayuela, A.; Soriano, M. L.; Carrillo-Carrión, C.; Valcárcel, M. Semiconductor and Carbon-Based Fluorescent Nanodots: The Need for Consistency. *Chem. Commun.* **2016**, *52*, 1311−1326.

(3) Bourlinos, A. B.; Stassinopoulos, A.; Anglos, D.; Zboril, R.; Karakassides, M.; Giannelis, E. P. Surface Functionalized Carbogenic Quantum Dots. *Small* **2008**, *4*, 455−458.

(4) Choi, Y.; Choi, Y.; Kwon, O.-H.; Kim, B.-S. Carbon Dots: Bottom-Up Syntheses, Properties, and Light-Harvesting Applications. *Chem. - Asian J.* **2018**, *13*, 586−598.

(5) Zhang, X.; Jiang, M.; Niu, N.; Chen, Z.; Li, S.; Liu, S.; Li, J. Natural-Product-Derived Carbon Dots: From Natural Products to Functional Materials. *ChemSusChem* **2018**, *11*, 11−24.

(6) Das, R.; Bandyopadhyay, R.; Pramanik, P. Carbon Quantum Dots from Natural Resource: A Review. *Mater. Today Chem.* **2018**, *8*, 96−109.

DOI: 10.1021/acs.accounts.8b00673
Acc. Chem. Res. XXXX, XXX, XXX−XXX

(7) Wu, Z. L.; Liu, Z. X.; Yuan, Y. H. Carbon Dots: Materials, Synthesis, Properties and Approaches to Long-Wavelength and Multicolor Emission. *J. Mater. Chem. B* **2017**, *5*, 3794−3809.
(8) Wang, Y.; Zhu, Y.; Yu, S.; Jiang, C. Fluorescent Carbon Dots: Rational Synthesis, Tunable Optical Properties and Analytical Applications. *RSC Adv.* **2017**, *7*, 40973−40989.
(9) Zheng, X. T.; Ananthanarayanan, A.; Luo, K. Q.; Chen, P. Glowing Graphene Quantum Dots and Carbon Dots: Properties, Syntheses, and Biological Applications. *Small* **2015**, *11*, 1620−1636.
(10) Wang, S.; Liu, N.; Su, J.; Li, L.; Long, F.; Zou, Z.; Jiang, X.; Gao, Y. Highly Stretchable and Self-Healable Supercapacitor with Reduced Graphene Oxide Based Fiber Springs. *ACS Nano* **2017**, *11*, 2066−2074.
(11) Goryacheva, I. Y.; Sapelkin, A. V.; Sukhorukov, G. B. Carbon Nanodots: Mechanisms of Photoluminescence and Principles of Application. *TrAC, Trends Anal. Chem.* **2017**, *90*, 27−37.
(12) Wang, R.; Lu, K.-Q.; Tang, Z.-R.; Xu, Y.-J. Recent Progress in Carbon Quantum Dots: Synthesis, Properties and Applications in Photocatalysis. *J. Mater. Chem. A* **2017**, *5*, 3717−3734.
(13) Yu, H.; Shi, R.; Zhao, Y.; Waterhouse, G. I. N.; Wu, L.-Z.; Tung, C.-H.; Zhang, T. Smart Utilization of Carbon Dots in Semiconductor Photocatalysis. *Adv. Mater.* **2016**, *28*, 9454−9477.
(14) Luo, Y.; Xia, X.; Liang, Y.; Zhang, Y.; Ren, Q.; Li, J.; Jia, Z.; Tang, Y. Highly Visible-Light Luminescence Properties of the Carboxyl-Functionalized Short and Ultrashort MWNTs. *J. Solid State Chem.* **2007**, *180*, 1928−1933.
(15) Strauss, V. Ecofriendly Carbon Nanomaterials for Future Electronic Applications. *Chem.* **2017**, *2*, 319−321.
(16) Strauss, V.; Schäfer, R. A.; Hauke, F.; Hirsch, A.; Guldi, D. M. Polyhydrogenated Graphene: Excited State Dynamics in Photo- and Electroactive Two-Dimensional Domains. *J. Am. Chem. Soc.* **2015**, *137*, 13079−13086.
(17) Robertson, J. Recombination and Photoluminescence Mechanism in Hydrogenated Amorphous Carbon. *Phys. Rev. B: Condens. Matter Mater. Phys.* **1996**, *53*, 16302−16305.
(18) Robertson, J. Photoluminescence Mechanism in Amorphous Hydrogenated Carbon. *Diamond Relat. Mater.* **1996**, *5*, 457−460.
(19) Marchon, B.; Gui, J.; Grannen, K.; Rauch, G. C.; Silva, S. R. P.; Robertson, J.; Ager, J. W., III Photoluminescence and Raman Spectroscopy in Hydrogenated Carbon Films. *IEEE Trans. Magn.* **1997**, *33*, 3148−3150.
(20) Xu, X.; Ray, R.; Gu, Y.; Ploehn, H. J.; Gearheart, L.; Raker, K.; Scrivens, W. A. Electrophoretic Analysis and Purification of Fluorescent Single-Walled Carbon Nanotube Fragments. *J. Am. Chem. Soc.* **2004**, *126*, 12736−12737.
(21) Sun, Y.-P.; Zhou, B.; Lin, Y.; Wang, W.; Fernando, K. A.; Pathak, P.; Meziani, M. J.; Harruff, B. A.; Wang, X.; Wang, H.; Luo, P. G.; Yang, H.; Kose, M. E.; Chen, B.; Veca, L. M.; Xie, S. F. Quantum-Sized Carbon Dots for Bright and Colorful Photoluminescence. *J. Am. Chem. Soc.* **2006**, *128*, 7756−7757.
(22) Qu, S.; Zhou, D.; Li, D.; Ji, W.; Jing, P.; Han, D.; Liu, L.; Zeng, H.; Shen, D. Toward Efficient Orange Emissive Carbon Nanodots through Conjugated Sp 2 -Domain Controlling and Surface Charges Engineering. *Adv. Mater.* **2016**, *28*, 3516−3521.
(23) Miao, X.; Qu, D.; Yang, D.; Nie, B.; Zhao, Y.; Fan, H.; Sun, Z. Synthesis of Carbon Dots with Multiple Color Emission by Controlled Graphitization and Surface Functionalization. *Adv. Mater.* **2018**, *30*, 1704740.
(24) Qu, S.; Wang, X.; Lu, Q.; Liu, X.; Wang, L. A Biocompatible Fluorescent Ink Based on Water-Soluble Luminescent Carbon Nanodots. *Angew. Chem., Int. Ed.* **2012**, *51*, 12215−12218.
(25) Sell, W. J.; Easterfield, T. H. LXXIII.—Studies on Citrazinic Acid. Part I. *J. Chem. Soc., Trans.* **1893**, *63*, 1035−1051.
(26) Wang, W.; Wang, B.; Embrechts, H.; Damm, C.; Cadranel, A.; Strauss, V.; Distaso, M.; Hinterberger, V.; Guldi, D. M.; Peukert, W. Shedding Light on the Effective Fluorophore Structure of High Fluorescence Quantum Yield Carbon Nanodots. *RSC Adv.* **2017**, *7*, 24771−24780.
(27) Strauss, V.; Margraf, J. T.; Dolle, C.; Butz, B.; Nacken, T. J.; Walter, J.; Bauer, W.; Peukert, W.; Spiecker, E.; Clark, T.; Guldi, D. M. Carbon Nanodots: Toward a Comprehensive Understanding of Their Photoluminescence. *J. Am. Chem. Soc.* **2014**, *136*, 17308−17316.
(28) Strauss, V.; Kahnt, A.; Zolnhofer, E. M.; Meyer, K.; Maid, H.; Placht, C.; Bauer, W.; Nacken, T. J.; Peukert, W.; Etschel, S. H.; Halik, M.; Guldi, D. M. Assigning Electronic States in Carbon Nanodots. *Adv. Funct. Mater.* **2016**, *26*, 7975−7985.
(29) Krysmann, M. J.; Kelarakis, A.; Dallas, P.; Giannelis, E. P. Formation Mechanism of Carbogenic Nanoparticles with Dual Photoluminescence Emission. *J. Am. Chem. Soc.* **2012**, *134*, 747−750.
(30) Strauss, V.; Marsh, K.; Kowal, M. D.; El-Kady, M. F.; Kaner, R. B. A Simple Route to Porous Graphene from Carbon Nanodots for Supercapacitor Applications. *Adv. Mater.* **2018**, *30*, 1704449.
(31) Margraf, J. T.; Strauss, V.; Guldi, D. M.; Clark, T. The Electronic Structure of Amorphous Carbon Nanodots. *J. Phys. Chem. B* **2015**, *119*, 7258−7265.
(32) Fu, M.; Ehrat, F.; Wang, Y.; Milowska, K. Z.; Reckmeier, C.; Rogach, A. L.; Stolarczyk, J. K.; Urban, A. S.; Feldmann, J. Carbon Dots: A Unique Fluorescent Cocktail of Polycyclic Aromatic Hydrocarbons. *Nano Lett.* **2015**, *15*, 6030−6035.
(33) Ehrat, F.; Bhattacharyya, S.; Schneider, J.; Löf, A.; Wyrwich, R.; Rogach, A. L.; Stolarczyk, J. K.; Urban, A. S.; Feldmann, J. Tracking the Source of Carbon Dot Photoluminescence: Aromatic Domains versus Molecular Fluorophores. *Nano Lett.* **2017**, *17* (12), 7710−7716.
(34) Wang, X.; Cao, L.; Lu, F.; Meziani, M. J.; Li, H.; Qi, G.; Zhou, B.; Harruff, B. A.; Kermarrec, F.; Sun, Y.-P. Photoinduced Electron Transfers with Carbon Dots. *Chem. Commun.* **2009**, 3774.
(35) Cadranel, A.; Strauss, V.; Margraf, J. T.; Winterfeld, K. A.; Vogl, C.; Đorđević, L.; Arcudi, F.; Hoelzel, H.; Jux, N.; Prato, M.; Guldi, D. M. Screening Supramolecular Interactions between Carbon Nanodots and Porphyrins. *J. Am. Chem. Soc.* **2018**, *140*, 904−907.
(36) Ferrer-Ruiz, A.; Scharl, T.; Haines, P.; Rodríguez-Pérez, L.; Cadranel, A.; Herranz, M. Á.; Guldi, D. M.; Martín, N. Exploring Tetrathiafulvalene-Carbon Nanodot Conjugates in Charge Transfer Reactions. *Angew. Chem., Int. Ed.* **2018**, *57*, 1001−1005.
(37) Arcudi, F.; Strauss, V.; Đorđević, L.; Cadranel, A.; Guldi, D. M.; Prato, M. Porphyrin Antennas on Carbon Nanodots: Excited State Energy and Electron Transduction. *Angew. Chem., Int. Ed.* **2017**, *56*, 12097−12101.
(38) Scharl, T.; Cadranel, A.; Haines, P.; Strauss, V.; Bernhardt, S.; Vela, S.; Atienza, C.; Gröhn, F.; Martín, N.; Guldi, D. M. Fine-Tuning the Assemblies of Carbon Nanodots and Porphyrins. *Chem. Commun.* **2018**, *54*, 11642−11644.
(39) Strauss, V.; Margraf, J. T.; Clark, T.; Guldi, D. M. A Carbon−carbon Hybrid − Immobilizing Carbon Nanodots onto Carbon Nanotubes. *Chem. Sci.* **2015**, *6*, 6878−6885.
(40) Hasenöhrl, D. H.; Saha, A.; Strauss, V.; Wibmer, L.; Klein, S.; Guldi, D. M.; Hirsch, A. Bulbous Gold−carbon Nanodot Hybrid Nanoclusters for Cancer Therapy. *J. Mater. Chem. B* **2017**, *5*, 8591−8599.
(41) Margraf, J. T.; Lodermeyer, F.; Strauss, V.; Haines, P.; Walter, J.; Peukert, W.; Costa, R. D.; Clark, T.; Guldi, D. M. Using Carbon Nanodots as Inexpensive and Environmentally Friendly Sensitizers in Mesoscopic Solar Cells. *Nanoscale Horiz* **2016**, *1*, 220−226.
(42) Bhattacharyya, S.; Ehrat, F.; Urban, P.; Teves, R.; Wyrwich, R.; Döblinger, M.; Feldmann, J.; Urban, A. S.; Stolarczyk, J. K. Effect of Nitrogen Atom Positioning on the Trade-off between Emissive and Photocatalytic Properties of Carbon Dots. *Nat. Commun.* **2017**, *8*, 1401.
(43) Zhang, P.; Wang, T.; Chang, X.; Zhang, L.; Gong, J. Synergistic Cocatalytic Effect of Carbon Nanodots and Co 3 O 4 Nanoclusters for the Photoelectrochemical Water Oxidation on Hematite. *Angew. Chem., Int. Ed.* **2016**, *55*, 5851−5855.
(44) Choi, Y.; Jeon, D.; Choi, Y.; Ryu, J.; Kim, B.-S. Self-Assembled Supramolecular Hybrid of Carbon Nanodots and Polyoxometalates for Visible-Light-Driven Water Oxidation. *ACS Appl. Mater. Interfaces* **2018**, *10*, 13434−13441.

DOI: 10.1021/acs.accounts.8b00673
Acc. Chem. Res. XXXX, XXX, XXX−XXX